Journal of Translational Medicine

RESEARCH

Open Access

Dynamic functional connectivity and gene expression correlates in temporal lobe epilepsy: insights from hidden markov models

Lu Qin[1†], Qin Zhou[1†], Yuting Sun[1], Xiaomin Pang[1], Zirong Chen[1] and Jinou Zheng[1*]

Abstract

Backgroud Temporal lobe epilepsy (TLE) is associated with abnormal dynamic functional connectivity patterns, but the dynamic changes in brain activity at each time point remain unclear, as does the potential molecular mechanisms associated with the dynamic temporal characteristics of TLE.

Methods Resting-state functional magnetic resonance imaging (rs-fMRI) was acquired for 84 TLE patients and 35 healthy controls (HCs). The data was then used to conduct HMM analysis on rs-fMRI data from TLE patients and an HC group in order to explore the intricate temporal dynamics of brain activity in TLE patients with cognitive impairment (TLE-CI). Additionally, we aim to examine the gene expression profiles associated with the dynamic modular characteristics in TLE patients using the Allen Human Brain Atlas (AHBA) database.

Results Five HMM states were identified in this study. Compared with HCs, TLE and TLE-CI patients exhibited distinct changes in dynamics, including fractional occupancy, lifetimes, mean dwell time and switch rate. Furthermore, transition probability across HMM states were significantly different between TLE and TLE-CI patients ($p < 0.05$). The temporal reconfiguration of states in TLE and TLE-CI patients was associated with several brain networks (including the high-order default mode network (DMN), subcortical network (SCN), and cerebellum network (CN). Furthermore, a total of 1580 genes were revealed to be significantly associated with dynamic brain states of TLE, mainly enriched in neuronal signaling and synaptic function.

Conclusions This study provides new insights into characterizing dynamic neural activity in TLE. The brain network dynamics defined by HMM analysis may deepen our understanding of the neurobiological underpinnings of TLE and TLE-CI, indicating a linkage between neural configuration and gene expression in TLE.

Keywords Temporal lobe epilepsy, Cognitive impairment, Dynamic functional connectivity, Hidden Markov model, Resting-state functional magnetic resonance imaging, Gene expression

[†]Lu Qin and Qin Zhou contributed equally to this work.

*Correspondence:
Jinou Zheng
jinouzheng@163.com
[1]Department of Neurology, The First Affiliated Hospital of Guangxi Medical University, Nanning 530021, China

Introduction

Temporal lobe epilepsy (TLE) is the most common type of focal epilepsy in adults, with approximately 40% of TLE being intractable [1]. TLE is a progressive disease and is associated with a decline in a wide range of cognitive abilities [2], although the majority of seizures can be controlled with anti-epileptic drugs. However, TLE patients often exhibit varying degrees of cognitive impairment, such as memory disorders, naming difficulties, executive function impairment, and attention disturbances [3], which may continue to worsen as the epilepsy progresses. Up to 50-80% of TLE patients exhibit impairments in at least one cognitive domain, with memory being the most common [4, 5]. Nonetheless, cognitive impairments are easily overlooked. Typically, by the time a decline in cognitive abilities is detected, significant brain damage has already spread due to a lack of timely treatment. These widespread damages can lead to a significant decline in the quality of life for TLE patients, sometimes even more debilitating than the epileptic seizures themselves [6]. Therefore, there is an urgent need for new objective techniques to reveal the underlying neuropathological mechanisms of early cognitive impairments in TLE patients.

Resting-state functional magnetic resonance imaging (rs-fMRI) is a non-invasive method widely used to study potential changes in brain function related to TLE and other brain diseases [7]. Traditional static functional connectivity (FC) analysis assesses the synchrony of fMRI signal fluctuations by calculating the correlation coefficients between time series of pre-defined brain regions [8]. Many rs-fMRI studies have identified disruptions in FC within and between brain networks in TLE patients, including the default mode network (DMN), frontoparietal network (FPN), and subcortical network (SCN) [9, 10]. These alterations in FC within and between brain functional networks are associated with cognitive impairments. However, FC studies rely on the assumption that resting-state FC is "stationary" during scanning [11]. This assumption overlooks the considerable variability of FC during rs-fMRI and may be outdated. Increasing evidence suggests that the human brain system is a complex dynamic system, and FC fluctuates over time during scanning [12]. Some studies have reported abnormal dynamic functional connectivity features observed in TLE patients [13, 14] or patients with cognitive impairments, highlighting the importance of this new direction in studying brain connectivity dynamics in the field of neuroimaging and its critical role in revealing mechanisms related to cognitive impairments in TLE patients.

Capturing the temporal variability of complex functional activities and connectivity patterns (i.e., spatial states) is crucial for understanding the dynamic organizational ways of the brain [15]. Temporal characteristics associated with recurring spatial states can be characterized by fractional occupancy (FO), the proportion of time spent in a specific functional activity or connectivity state; lifetimes (LT), the amount of time spent in a specific state; mean dwell time (MDT), calculated as the average amount of time spent in a specific state; switch rate (SR), measuring the overall frequency of transitions between different functional states; and transition probability (TP), a core metric of the hidden Markov model (HMM), representing the probability of transitions between all pairs of HMM states [16]. These temporal-spatial measures, known as spatiotemporal metrics, of specific brain connections' dynamic patterns have been shown to be related to thought processing as well as specific cognitive and emotional states [17]. Moreover, changes in brain dynamics patterns are associated with Alzheimer's disease [18], isolated syndrome [19] and schizophrenia [20].

The sliding window method is widely utilized to analyze fluctuations in brain dynamics [21]. Using the sliding window method, abnormal connectivity in the DMN, sensory-motor network (SMN), and SCN has often been found in our previous rs-fMRI studies [22] and other studies involving TLE patients [23]. However, the sliding window method has its limitations [24]. It relies on a fixed window size, with predetermined dimensions and step increments, which are critical parameters. Choosing an optimal window size is crucial, as too long a window will restrict the visualization of rapid dynamics, while too short a window will miss enough data to perform a reliable network estimation [25]. The HMM effectively addresses these challenges by characterizing brain activity as a sequence of distinct states inferred from resting data [26]. Previous research has shown that HMM is capable of capturing the dynamics of brain activity on the smallest time scales [27]. Furthermore, previous studies have confirmed that rapid changes in brain activity are far from random; therefore, HMM helps to provide a richer description of the dynamic nature of brain activity in central nervous system diseases in a short period [28].

Brain activity is regulated by genes, and brain gene expression profiles assist in linking brain activity with genes [29]. The Allen Human Brain Atlas (AHBA) dataset is extensively utilized to investigate the relationship between gene expression and brain patterns [30]. Transcriptomic neuroimaging association analysis can uncover the molecular foundation of disease-related alterations. For example, Amanda et al. described dynamic connectivity patterns in different forms of autism spectrum disorder (ASD), revealing different molecular signaling mechanisms in different ASD subgroups [31]. Analysis by Ling et al. combining neuroimaging and transcription data suggests that genes related to neurovascular unit integrity and synaptic plasticity may drive changes in brain metabolism, thereby

mediating the genetic risk of TLE [32]. However, the underlying molecular mechanisms associated with the dynamic neural structure of TLE remain unclear.

The purpose of this study is to conduct HMM analysis on rs-fMRI data from TLE patients and an HC group in order to explore the intricate temporal dynamics of brain activity in TLE patients with cognitive impairment (TLE-CI). Additionally, the study aims to examine the gene expression profiles associated with the dynamic modular characteristics in TLE patients using the AHBA database. The analysis focused on identifying specific patterns of cross-state transitions, inter-network brain connectivity, and gene mechanisms, aiming to provide new insights into TLE and TLE-CI.

Materials and methods

Participants

Participants diagnosed with TLE at the First Affiliated Hospital of Guangxi Medical University from January 2019 to December 2023 were included in the study. Adhering to the criteria of the International League Against Epilepsy (ILAE) delineated in 1981, 1989, and 2017 [33], we ensured a meticulous diagnostic process. Eligible participants included those who (1) received a confirmed TLE diagnosis, (2) followed a stable antiepileptic drug regimen, and (3) were verified as right-handed. Exclusion criteria encompassed individuals with (1) secondary epilepsy attributable to identifiable cranial structural anomalies such as trauma, tumors, or vascular irregularities, (2) a history of neurological or psychiatric conditions, or other severe physical illnesses, (3) previous substance or alcohol abuse, (4) contraindications for MRI procedures, or (5) insufficient adherence to the study protocol or subpar MRI data quality. It is important to note that hippocampal atrophy and sclerosis, common in TLE patients, were not grounds for exclusion in this study. We also included a control group of 35 neurologically and psychiatrically healthy individuals to provide a baseline for neuroimaging comparisons. This group was demographically matched to the patient cohort and had undergone a comprehensive health screening. The study's protocols were sanctioned by the Ethics Committee of the First Affiliated Hospital of Guangxi Medical University, and informed consent was obtained from all participants.

Neuropsychological testing

All participants diagnosed with TLE underwent a comprehensive neuropsychological evaluation. Their cognitive functions, including language, memory, attention, visual-spatial skills, and executive abilities, were assessed using the Montreal Cognitive Assessment (MoCA) [34]. Participants scoring below 26 were classified as TLE patients having cognitive impairment (TLE-CI), while a score greater than 26 was considered to have TLE patients with normal cognitive function (TLE-CN).

MRI data acquisition

MRI data were collected using a 3.0-Tesla scanner (Philips, Netherlands). Participants underwent a 450-second rs-fMRI session, resulting in the capture of 225 cerebral volumes. High-resolution sagittal T1-weighted images were obtained, followed by the acquisition of axial T2 fluid-attenuated inversion recovery (FLAIR) sequences to identify and remove any subtle brain lesions that were not clinically apparent. Detailed methods for the collection of rs-fMRI data and T1-weighted structural images are provided in the supplementary materials.

Image preprocessing

The DPABI software, operating in the MATLAB R2018b environment, was utilized for the extraction and preprocessing of rs-fMRI data. The process commenced with the conversion of DICOM imaging files to NIfTI format. Detailed preprocessing steps are available in the supplementary materials.

Hidden Markov model

The HMM posits that fluctuations in brain region time series can be condensed into a finite set of latent states, each representing a transient state that may persist or transition to another. The model computes the probability of being in a given state and the transition likelihood between states. Central to the HMM analysis was the segmentation of each participant's brain into 116 regions of interest (ROIs) using the Automated Anatomical Labeling (AAL) atlas, the averaging of time series data within ROIs to generate a composite time series, the standardization of these series, and their amalgamation into a unified dataset. From this dataset, the HMM discerned distinct, recurrent states, each exhibiting unique statistical characteristics. To determine the optimal number of HMM states, we assessed the minimum free energy and the occupancy rate of the middle segment. Finally, we derived measures from the HMM states—including FO, LT, MDT, SR, and TP—to capture the temporal dynamics within subjects (supplementary materials).

Gene expression data preprocessing

The AHBA (http://human.brain-map.org) provides normalized microarray expression data from six donated human brains (all without known neuropsychiatric or neuropathological history), including more than 20,000 genes across 3,702 brain tissue samples. The gene expression data was preprocessed using the abagen toolbox(https://www.github.com/netneurolab/abagen). Detailed preprocessing steps are provided in the supplementary materials. Finally, the expression values for

each gene were also normalized across samples using the scaled robust sigmoid method. The resulting gene expression matrix (1,938 samples × 15,633 genes) was used for subsequent analyses.

Transcription-neuroimaging association analysis

Based on the AHBA gene expression data and mean activation of HMM states 3 with temporal characteristics, spatial associations between gene expression and the mean activation of HMM state 3 were investigated. The mean value of the voxels within a 6-mm radius sphere, centered on the coordinate of each tissue sample, was extracted from the mean activation of HMM state 3. Subsequently, spatial correlations between gene expression and the mean activation of HMM state 3 in TLE were analyzed using Pearson's correlation method. Multiple comparisons were adjusted by the Bonferroni method ($P < 0.05/15633 = 3.20 \times 10^{-6}$). Based on previous research, we downloaded the TLE gene expression profile [35]. Finally, the genes identified after multiple comparison adjustments, which intersected with the TLE expression gene profile, were defined as genes associated with the dynamic state of TLE.

Enrichment analysis

The Gene Ontology (GO) enrichment analysis, which includes biological processes (BP), molecular functions (MF), and cellular components (CC), as well as the Kyoto Encyclopedia of Genes and Genomes (KEGG) enrichment analysis, was conducted using the DAVID database (https://david.ncifcrf.gov/) for genes associated with dynamic states. The significance threshold was set at $p < 0.05$ (FDR corrected).

The protein-protein interaction (PPI) network for the genes related to dynamic states was constructed using the STRING database (https://string-db.org/). The confidence level was set to 0.9, while other parameters were left at their default values. Hub nodes in the PPI network were identified using Cytoscape. The degree centrality algorithm was used to identify five hub genes in the PPI network, which were considered the most crucial genes in biological functions.

Statistical analysis

The SPSS 25.0 software package (SPSS, Inc., Chicago, IL, USA) [36] and GRETNA [37]were used in this study. Continuous variables were presented as mean ± standard deviation (SD), while categorical variables were expressed as frequency counts. For continuous data, comparisons were made using independent sample t-tests or one way ANOVA, while chi-square tests were utilized to analyze categorical data.

To examine the FO, LT, MDT and SR of HMM states, two-tailed two-sample t-tests were used to compare TLE patients with HCs and TLE-CI against TLE-CN. A false discovery rate (FDR) correction was applied to account for multiple testing, with a significance threshold set at $p < 0.05$.

A nonparametric permutation test was used to examine the TP of HMM states between TLE patients and HCs, as well as between TLE-CI and TLE-CN. A total of 5,000 permutations were conducted to establish a null distribution of dynamic global differences between the groups for each state, and p-values were calculated accordingly.

Spearman's correlation analysis was used to evaluate the relationship between MoCA scores and changes in FO, LT, and MDT of HMM states in TLE-CI. A significance threshold of $p < 0.05$ was applied, with adjustments made for confounding factors such as age, sex, and education level.

Results

Demographic and clinical data

This study ultimately analyzed 84 TLE patients and 35 HCs. Table 1 displays the demographic and clinical characteristics of both TLE patients and HCs. There were no significant differences among the three groups in terms of age, gender, and education level. However, there were notable differences in MoCA scores between the TLE-CI, TLE-CN, and HCs.

Aberrant dynamics for each HMM state in TLE patients

Firstly, the rs-fMRI data of 119 subjects (including 84 TLE subjects and 35 HCs) were used to estimate the HMM states. We observed that HMM state 5 exhibited the minimum free energy and intermediate fraction occupancy. Consequently, based on these findings, this study ultimately estimated 5 HMM states (Fig. 1).

In the HMM, FO was utilized to investigate the temporal characteristics of TLE. Compared to HCs, the FO of HMM state 3was significantly lower in TLE patients ($p = 8.6^{*}10^{-7}$) (Fig. 2a). There were no significant differences in the FO of the remaining HMM states between TLE patients and HCs (Fig. 2a). The LT of HMM state 3 was significantly shorter in TLE patients ($p = 1.2^{*}10^{-4}$) (Fig. 2b), and MDT of HMM state 3 was also significantly shorter for TLE patients ($p = 1.2^{*}10^{-4}$) (Fig. 2c). However, the FO, LT, and MDT of HMM states showed no significant differences between TLE-CI and TLE-CN. (Fig. 2d-e).

Aberrant transition patterns between HMM

The SR of TLE patients was significantly higher than that of HCs ($p = 0.010$) (Fig. 3a), indicating distinct network dynamic patterns between TLE patients and HCs during the entire scan. Furthermore, permutation analysis (5000 permutations) revealed significant group differences in the TP of HMM states between TLE patients and HCs.

Table 1 Demographic characteristics and clinical features of patients with TLE and HCs

Variables	TLE whole sample (n = 84)	TLE-CI(n = 30)	TLE-CN(n = 54)	HCs(n = 35)	P-value
Demographic characteristics					
Age(years)	31.76 ± 9.53	33.47 ± 11.72	30.81 ± 8.03	28.71 ± 7.55	0.108[b]
Gender (M/F)	30/54	10/20	20/34	13/22	0.934[a]
Education(years)(range)	12.97 ± 4.03	11.93 ± 3.18	13.56 ± 4.36	13.63 ± 3.06	0.116[b]
Clinical characteristics					
Onset of epilepsy, (years)	16.18 ± 13.33	15.50 ± 7.26	16.56 ± 15.78	NA	0.730[c]
Duration of epilepsy, (years)	10.73 ± 7.04	10.83 ± 7.45	10.15 ± 6.70	NA	0.668[c]
AEDs (mono-/polytherapy)	27/57	5/25	22/32	NA	0.024[a*]
MoCA total score	26.21 ± 2.79	23.23 ± 2.32	27.87 ± 1.21	28.63 ± 1.57	0.000[b*]

HC, healthy control; TLE-CI, TLE patients with cognitive impairment; TLE-CN, TLE patients with cognitive normal; AEDs, antiepileptic drugs; NA, not available; MoCA, Montreal Cognitive Assessment; M, male; F, female; M ± SD, mean ± standard deviation; The results of comparing P values among TLE-CI, TLE-CN, and HCs. *, post-hoc comparison revealed a significant difference between TLE-CI, TLE-CN and HCs

[a]P was calculated using the chi-square test

[b]P was calculated using an ANOVA

[c]P was calculated using two independent sample t-tests

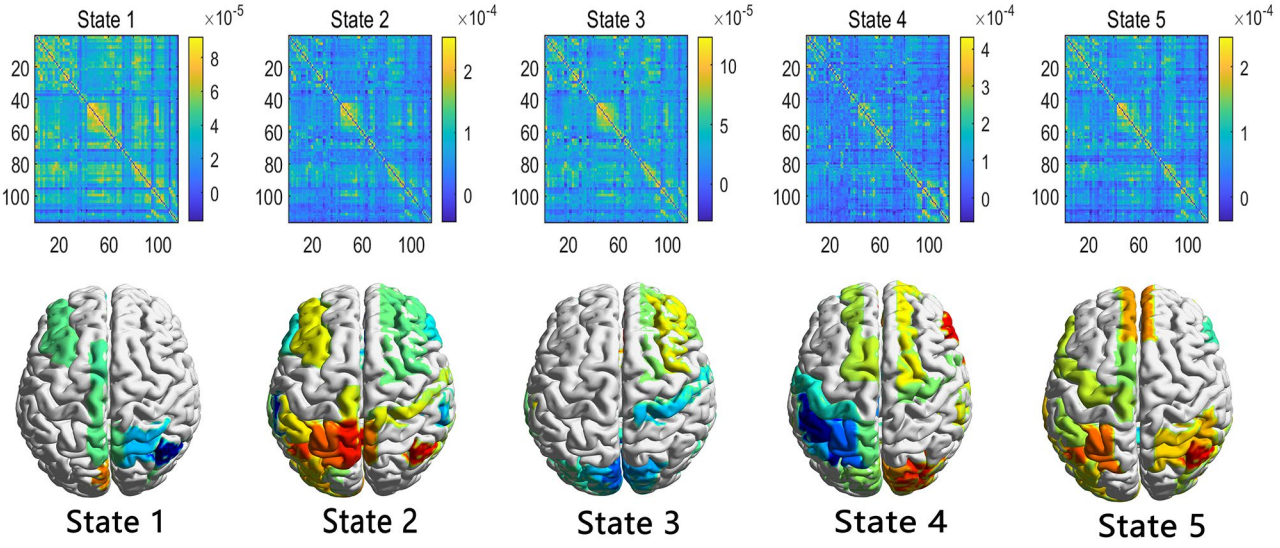

Fig. 1 5 HMM states. HMM, hidden Markov model

Significant group differences in TP between HMM states are shown in Fig. 3b. Compared to HCs, patients with TLE exhibited significantly increased TP from HMM states 2, 4, and 5 to state 1, from states 1 and 2 to state 2, from states 4 and 5 to state 3, from states 2, 3, 4, and 5 to state 4, and from states 1, 2, 3, 4, and 5 to state 5 (state 2 to 1: p=0.0316; state 4 to 1: p=0.0070; state 5 to 1: p=0.0098; state 1 to 2: p=0.0012; state 2 to 2: p=0.0100; state 4 to 3: p=0.0150; state 5 to 3: p=0.0112; state 2 to 4: p=0.000; state 3 to 4: p=0.0032; state 4 to 4: p=0.000; state 5 to 4: p=0.0110; state 1 to 5: p=0.0386; state 2 to 5: p=0.000; state 3 to 5: p=0.0038; state 4 to 5: p=0.0028; state 5 to 5: p=0.0000). The TP from HMM states 1, 3 to state 3 was significantly reduced in TLE patients (state 1 to 3: p=0.0000; state 3 to 3: p=0.0042). These findings suggest significant abnormal transition patterns between HMM states in TLE patients.

The SR was not significantly different between TLE-CI and TLE-CN (p=0.098) (Fig. 3c), indicating similar stable network dynamic patterns in both groups. However, significant group differences in TP between HMM states are shown in Fig. 4d. Compared to TLE-CN, the TP from HMM states 3,4 and 5 to state 4, from state 2 to state 2, and from state 2 to state 3 increased significantly for TLE-CI (state 3 to 4: p=0.0424; state 4 to 4: p=0.0458; state 5 to 4: p=0.0468; state 2 to 2: p=0.0104; state 2 to 3: p=0.0482). These results suggest significant aberrant transition patterns between HMM states in TLE-CI.

Brain activation maps of states

In patients with TLE, spatial activation maps reveal that the predominant state of the large-scale global brain network is State 3 (Fig. 4a). This state is characterized by enhanced activity primarily within the DMN region

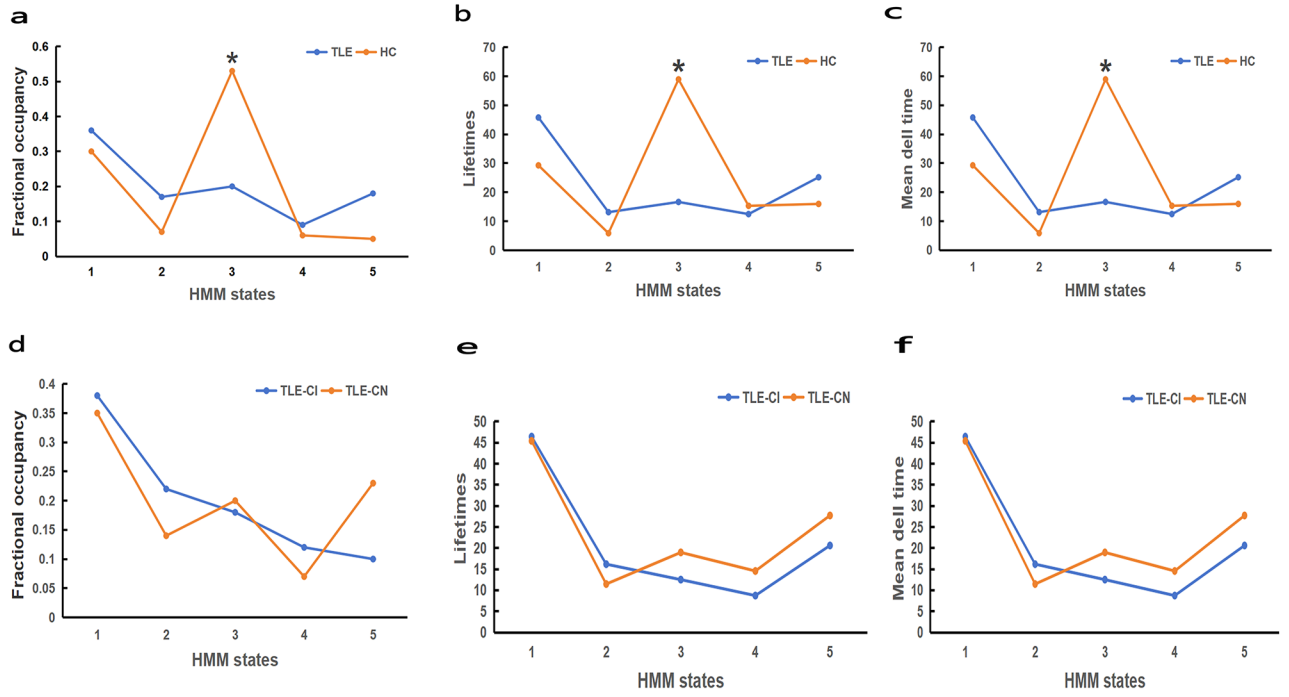

Fig. 2 Differences in dynamic indicators. (**a**-**c**) Significant differences in FO, LT and MDT of each HMM state between TLE patients and HCs. (**d**-**f**) Significant difference in FO, LT and MDT of each HMM state between TLE-CI and TLE-CN. All temporal properties were evaluated using a two-tailed, two-sample t-test. *Significant group differences ($p < 0.05$). TLE, temporal lobe epilepsy; HCs, healthy controls; TLE-CI, temporal lobe epilepsy with cognitive impairment; TLE-CN, temporal lobe epilepsy with normal cognitive; FO, fractional occupancy; LT, Lifetimes; MDT, Mean dwell time

(including the frontal lobe, parietal lobe, and cingulate gyrus). Conversely, reductions in activity are observed in the occipital lobe, subcortical regions, and cerebellum. The spatial activation map of the large-scale global brain network state in TLE-CI is primarily dominated by state 2 (Fig. 4b). HMM state 2 exhibits increased activation in the parietal lobe and cerebellum, while decreased activation in the temporal lobe and subcortical area.

Correlation analysis

There was no significant correlation between the dynamic indicators of each HMM state and the MoCA scores for patients with TLE ($p > 0.05$). Similarly, for TLE-CI, there was also no significant correlation between the dynamic indicators of each HMM status and MoCA scores ($p > 0.05$).

HMM States-related genes in TLE

Pearson's correlation analysis was conducted to determine the relationships between the mean activation of HMM states with dynamic temporal characteristics (state 3) and gene expressions. After conducting multiple comparisons and corrections, we identified 3,815 genes. Ultimately, by intersecting the gene expression profile of TLE genes discovered in previous studies with the genes obtained through multiple comparisons and corrections, a total of 1,580 genes were identified and defined as TLE dynamic state-related genes.

Enrichment analysis

Using the DAVID database, we compared GO pathways with the genes related to TLE dynamic states. The results of the GO enrichment analysis are illustrated in Fig. 5a, highlighting significantly enriched categories in BP, CC, and MF. Key BP includes "signal transduction", "cell adhesion", and "axon guidance". Enriched CC involves "cytosol", "cytoplasm", "presynaptic" and "postsynaptic membranes". For MF, categories such as "ion channel activity", "protein binding", and "calcium ion binding" show notable enrichment. The KEGG enrichment analysis of significant genes reveals notable pathways including "circadian entrainment", "morphine addiction", and "calcium signaling pathway" (Fig. 5b).

PPI network analysis

Based on 1,580 TLE dynamic states-related genes, we performed the PPI network analysis. We constructed a network consisting of 669 edges, which is significantly higher than the expected 540 edges. We found that the proteins coded by PIK3CA, PIK3CB, PIK3CD, CTNNB1 and ITGB1 were the top five hub genes in the PPI network (Fig. 6).

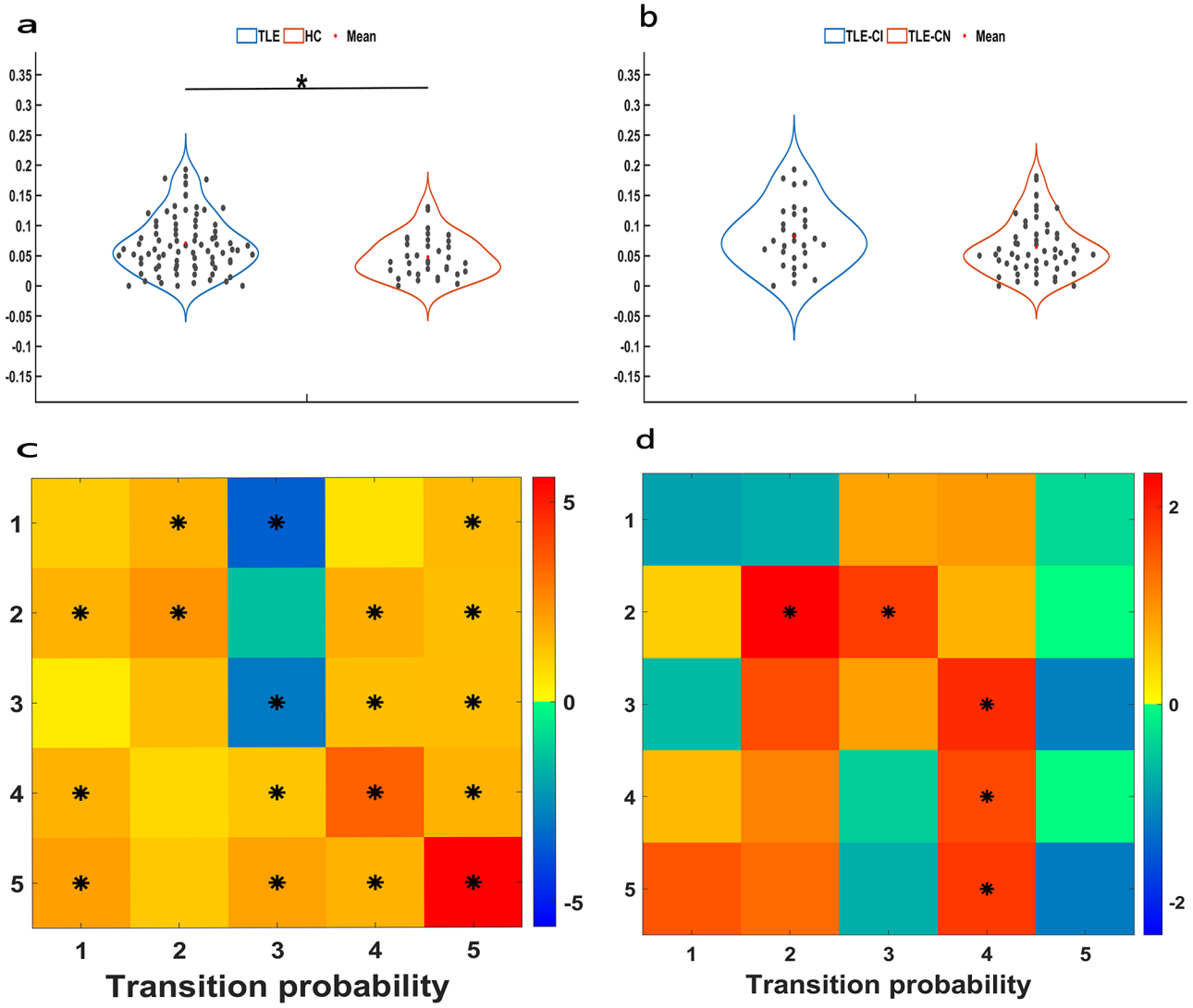

Fig. 3 Alterations in SR and TP. (**a**) Alterations in SR between TLE patients and HCs. (**c**) The significant alterations in TP between TLE patients and HCs. * represents a significant increase in TLE patients compared with HCs. Red represents a significant increase in TLE patients compared with HCs, and blue represents a significant decrease in TLE patients compared with HCs. (**b**) Alterations in SR between TLE-CI and TLE-CN. (**d**) The significant alterations in TP between TLE-CI and TLE-CN. Red represents a significant increase in TLE-CI compared with TLE-CN, and blue represents a significant decrease in TLE-CI compared with TLE-CN. Significant group differences were evaluated using a permutation test with 5000 permutations. *$p < 0.05$. TLE, temporal lobe epilepsy; HCs, healthy controls; TLE-CI, temporal lobe epilepsy with cognitive impairment; TLE-CN, temporal lobe epilepsy with normal cognitive; SR, switch rate; TP, transition probability

Discussion

In this study, we conducted HMM analysis on rs-fMRI data from TLE patients and an HC group to explore the intricate temporal dynamics of brain activity in TLE-CI. Additionally, we examined the gene expression profiles associated with the dynamic modular characteristics in TLE patients using the AHBA database. We identified five unique spatial states characterized by functional connectivity and mean functional activity across our study sample. Dynamic measurements showed that compared to HCs, TLE patients had shorter LT, MDT, and lower FO in state 3, which was characterized by higher activity in the DMN, SMN, and SCN. There was no significant difference in dynamic measures between TLE-CI and TLE-CN. Additionally, we found significant differences in SR and TP between TLE patients and HCs. No significant differences in SR were found between TLE-CI and TLE-CN, but TP differed significantly. Our findings suggest that under rs-fMRI, TLE-CI patients demonstrate cerebellar network reorganization, potentially reflecting compensatory changes in the brain in response to disease impact. However, we did not find a correlation between dynamic network abnormalities and neurocognitive performance. Additionally, a total of 1580 genes associated with TLE HMM states activation were identified. The enrichment analysis indicated that these genes, related to

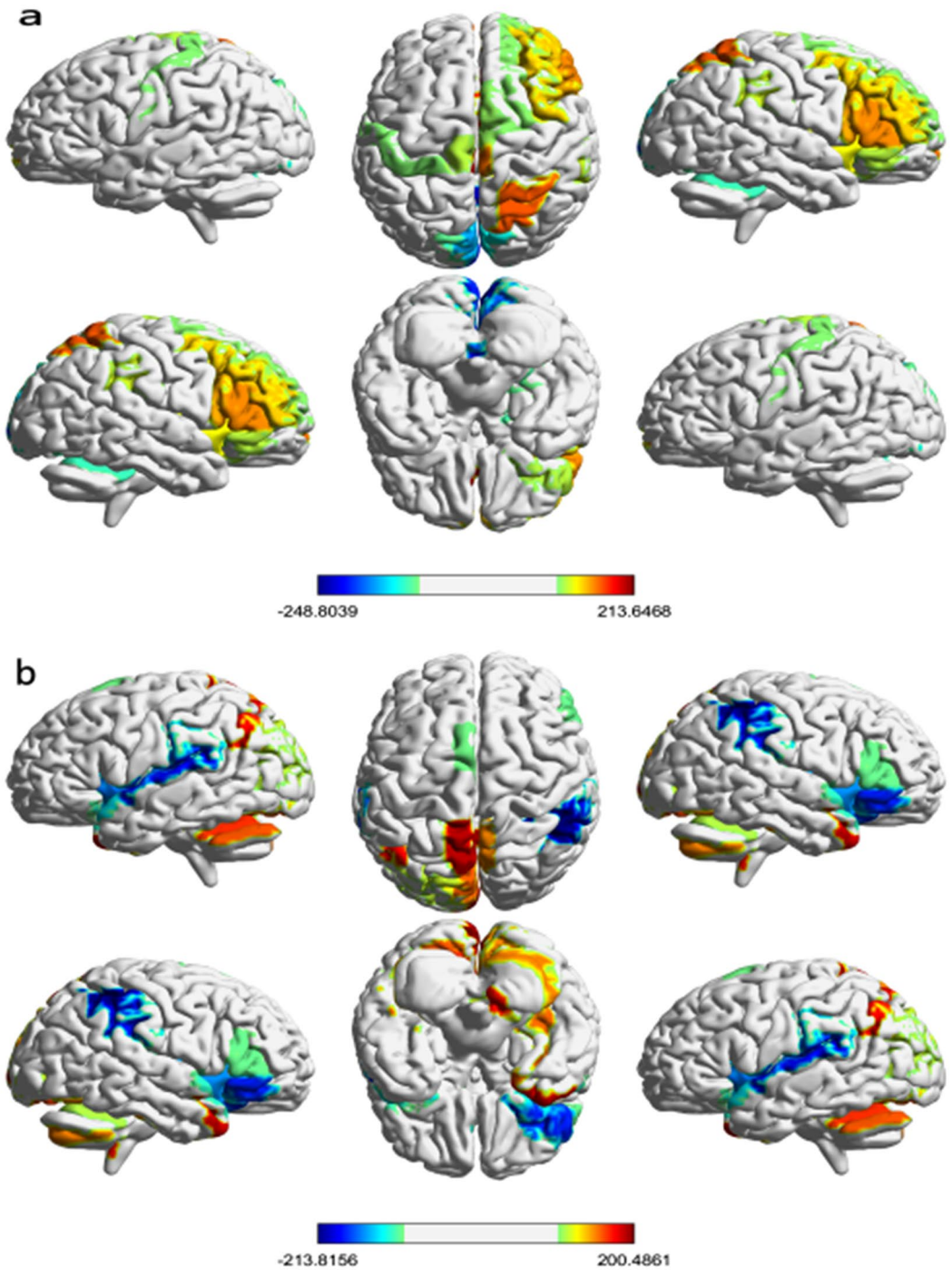

Fig. 4 Brain activation maps of states. (**a**) Mean activation distribution of state 3 predominantly induced by TLE. (**b**) Mean activation distributions of state 2 predominantly induced by TLE-CI

the dynamic states of TLE, were ontologically enriched for several terms pertinent to TLE, such as presynaptic/postsynaptic embranes, ion channel activity, and protein binding. These findings unveiled the dynamic neural configuration of TLE based on rs-fMRI data, aiding in the comprehension of specific TLE mechanisms from an integrative perspective.

Brain network dynamics in TLE

We revealed the neural dynamics in TLE and those with cognitive impairment using HMM. Compared to HCs,

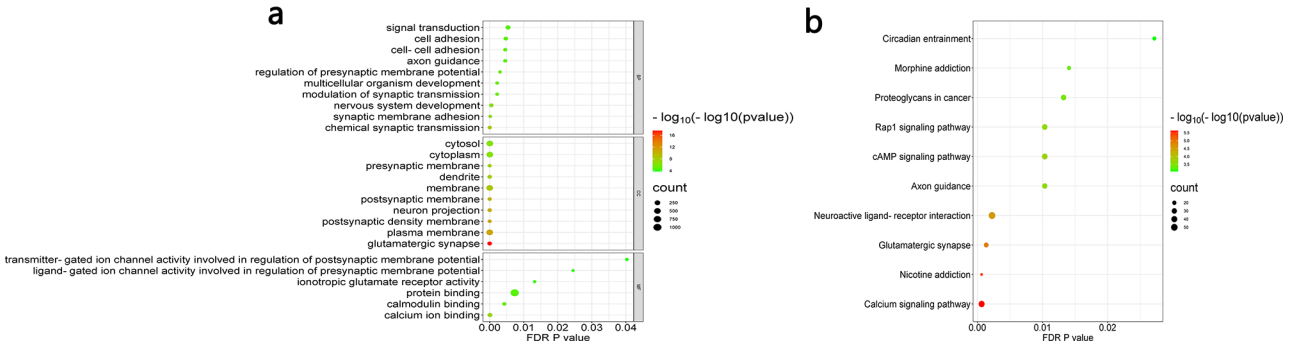

Fig. 5 Results derived from GO and KEGG enrichment analysis. The size of the circle represents the number of genes involved in an ontology term and the color of each circle represents the significance level. GO, GeneOntology; KEGG, Kyoto Encyclopedia of Genes and Genomes; BP, Biological processes; MF, Molecular functions; CC, Cellular components

the brain dynamics of TLE patients have changed. We identified five unique brain activity states, indicating that FC in patients with TLE fluctuates over time instead of remaining static. We then evaluated the temporal distribution of these states. The results showed significant differences in the overall distribution of brain states between TLE patients and HCs, particularly in terms of FO, LT, and MDT, consistent with previous research findings [38, 39]. Similar observations were also observed in rs-fMRI studies of TLE animal models [40]. These differences suggest that the neural network dynamics in TLE patients are characterized by reductions in LT and MDT, as well as diminished FO. These findings may reflect a decrease in the stability of network configurations and a weakening of inter-regional connectivity. Furthermore, although TLE-CI showed a trend toward increased state occupancy rate and reduced duration compared to TLE-CN, these differences were not statistically significant, suggesting that TLE-CI patients may have similar changes in dynamic functional connectivity as TLE-CN. However, we were unable to establish a direct correlation between these dynamic network anomalies and neurocognitive performance, considering the compensatory effect of the TLE-CI [41].

The complex dynamic system of the human brain underpins cognitive functions through consistent and fluid state transitions. Comprehending these transitions is pivotal for understanding functional plasticity in TLE-affected brains with cognitive deficits. We analyzed SR for all five HMM states, indicating the frequency of transitions between states [42]. The results showed that the SR and TP of brain states between TLE patients and HC were significantly different, with TLE patients having higher SR than HC, indicating that TLE patients exhibit an unstable pattern of transitions [43]. More specifically, HMM analysis can capture most of the information contained in the data.

Brain network dynamics in TLE-CI

Furthermore, dynamic distortions were observed in TLE-CI. There was no significant difference in SR between TLE-CI and TLE-CN, indicating similar patterns of transitions in brain connectivity. However, there were significant group differences in TP, suggesting that TLE-CI have undergone significant changes in their brain state transition patterns. This inflexibility in state transitions may be related to the pathophysiology of TLE-CI [44].

Based on spatial activation maps of large-scale whole-brain network states induced by TLE, our results show high activation in the DMN, SCN, and SMN, with low activation in the visual network (VN) and CN. For large-scale whole-brain network states induced by TLE-CI, our results indicate low activation in the SMN and high activation in the CN. These findings are consistent with previous evidence that TLE patients exhibit abnormal static and dynamic network interactions in the DMN, VN, SMN, and CN [45, 46]. The DMN, VN, and SMN networks, which are widely studied in TLE patients, exhibit abnormal connectivity across a broad range of TLE pathophysiology [47, 48]. Notably, we observed high CN activation in TLE-CI, which aligns with the results from a previous study [49]. Although classically thought of as a motor circuit, the cerebellum is now understood to contribute to a wide variety of cognitive functions through its dense interconnections with the neocortex, the center of brain cognition [50]. Some studies have shown that the structural and functional changes in the cerebellum of TLE patients are associated with cognitive impairment [51, 52]. In summary, these findings suggest that the CN is also important in TLE and may be a promising biomarker for studying TLE-CI. Reduced FNC reflects network functional impairment, while increased FNC is attributed to compensatory mechanisms or reorganization following microstructural damage in the brain.

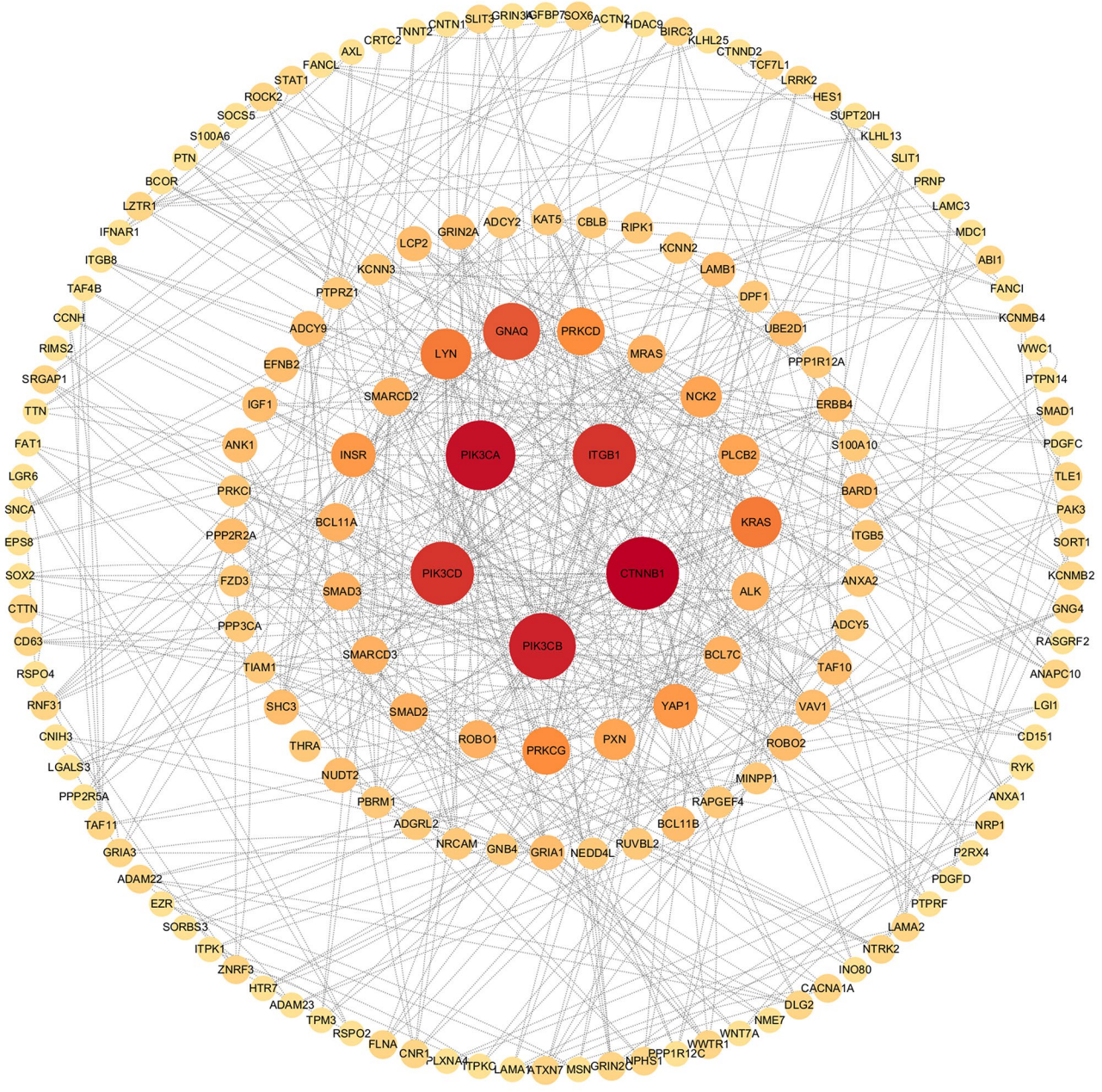

Fig. 6 PPI network constructed by the TLE dynamic states-related genes. The size and color of the circles indicate the magnitude of degree centrality. TLE, temporal lobe epilepsy; PPI, Protein-protein interaction

Link between neural configuration and gene expression

We linked the activation of HMM states with dynamic temporal characteristics in TLE to gene expression levels. TLE is a complex disorder influenced by elements such as synaptic connectivity, receptor functions, and ion channel abnormalities, which have been shown to predispose individuals to TLE [53]. Recent advances in human imaging genetics provide insights into exploring genes associated with brain functional or structural measurements. By using Pearson's correlation analysis, we identified 1,580 genes related to the dynamic state of TLE. Enrichment analysis revealed that these genes were enriched in several ontological terms, including cytoplasm, presynaptic and postsynaptic membranes, ion channel activity, protein binding, and calcium ion binding. Changes in the structure and function of synaptic connections in the brain have also been confirmed in TLE patients and animal models [54]. Epilepsy is caused by abnormal electrical currents passing through the membranes of neuronal cells, facilitated by numerous ion channels. The dysfunction of these ion channels is the basis for the excessive excitation of neurons leading

to epilepsy [55]. Therefore, it is not surprising that ion channel-related terms appear in the ontological terms. Notably, KEGG pathway analysis identified critical pathways such as circadian entrainment, morphine addiction, and the calcium signaling pathway, which have been implicated in epilepsy and neurological disorders in prior studies [56]. Seizures exhibit sleep-wake and circadian patterns in various epilepsies and, in turn, disrupt sleep and circadian rhythms. The resulting sleep deprivation may lead to disease progression and even epilepsy-related deaths [57]. Although there is not enough evidence to suggest "TLE-specific" genes, our study provides a potential perspective for understanding TLE from multiple scales. Our research findings expand the landscape of emerging molecular pathways in TLE and suggest that genes related to the dynamic state of TLE warrant further investigation.

PPI network

Additionally, enrichment analysis revealed that TLE dynamic states-related genes were mainly enriched in presynaptic/postsynaptic embranes, ion channel activity, and protein binding, indicating that multiple pathways were contributed to brain dynamics in TLE. PPI network analysis revealed a network with 669 edges, significantly surpassing the expected 540 edges, indicating a highly interconnected landscape of protein interactions. Notably, the hub genes PIK3CA, PIK3CB, and PIK3CD are subtypes of type I PI3K, which encode different catalytic subunits. PI3K (phosphatidylinositol-3-kinase) is an important intracellular signaling enzyme that plays a crucial role in various cellular functions, including cell growth, proliferation, differentiation, survival, and motility. PI3K activates downstream signaling molecules such as AKT (protein kinase B) and mTOR (mammalian target of rapamycin) pathways by generating phosphatidylinositol (3,4,5)-triphosphate (PIP3) during signal transduction, thereby regulating many cellular processes [58]. The PI3K/AKT signaling pathway is one of the pathways in epilepsy and plays an important role in the pathogenesis of epilepsy [59]. Additionally, CTNNB1 and ITGB1 as top hub genes suggest a more pronounced role for Wnt signaling and integrin-mediated pathways in TLE than previously recognized, providing novel insights that could inform future therapeutic strategies [60]. Future studies also need to explore causal effects of these genes in TLE.

This study has several limitations. The sample sizes of TLE-CI and TLE-CN groups were unequal. Future research should aim to increase the sample size and incorporate longitudinal measures to explore group differences related to dynamic characteristics. Patients received various types, doses, and durations of antiepileptic drug treatment, which could affect the results of the current study. The functional MRI scans for each participant were relatively short in duration. To mitigate this limitation, we concatenated the time series data from all participants and applied the HMM model to the resulting extended dataset. This approach enabled us to capture sufficient temporal information to address the issue of short scan durations. Furthermore, although we linked the activation of TLE dynamic states to transcriptional data to advance our understanding of the relationship between molecular mechanisms and neural dynamics in TLE, the transcription-neuroimaging associations study could not provide any evidence of causation, as it is based solely on correlation.

Conclusions

This study provides new insights into characterizing dynamic neural activity in TLE. The brain network dynamics defined by HMM analysis may deepen our understanding of the neurobiological underpinnings of TLE and TLE-CI, indicating a linkage between neural configuration and gene expression in TLE.

Abbreviations

AAL	Automated Anatomical Labeling
AHBA	Allen Human Brain Atlas
ASD	Autism spectrum disorder
BP	Biological processes
CC	Cellular components
CN	Cerebellum network
DMN	Default mode network
FC	Functional connectivity
FDR	False discovery rate
FLAIR	Fluid-attenuated inversion recovery
FO	Fractional occupancy
FPN	Frontoparietal network
GO	Gene Ontology
HCs	Healthy controls
HMM	Hidden Markov model
ILAE	International League Against Epilepsy
KEGG	Kyoto Encyclopedia of Genes and Genomes
LT	Lifetimes
MF	Molecular functions
MoCA	Montreal Cognitive Assessment
MRI	Magnetic resonance imaging
PPI	Protein-protein interaction
ROIs	Regions of interest
rs-fMRI	Resting-state functional magnetic resonance imaging
SCN	Subcortical network
SD	Mean ± standard deviation
SMN	Sensory-motor network
SR	Switch rate
TLE	Temporal lobe epilepsy
TLE-CI	TLE patients with cognitive impairment
TLE-CN	TLE patients with normal cognitive function
TP	Transition probability
VN	Visual network

Supplementary Information

The online version contains supplementary material available at https://doi.org/10.1186/s12967-024-05580-2.

Supplementary Material 1: Fig. S1. The choice of the number of HMM states. HMM, hidden Markov model

Acknowledgements
We thank all participants for their time and participation.

Author contributions
Lu Qin designed the study and wrote the original draft. Qin Zhou carried out the data processing. Yuting Sun conducted the statistical analyses. Xiaomin Pang and Zirong Chen drafted the manuscript. All authors interpreted the data. Jinou Zheng revised the manuscript. All authors read and approved the final manuscript.

Funding
This study was funded by a grant from the National Natural Science Foundation of China (no. 81560223).

Data availability
The data of this study is available from the corresponding author upon reasonable request.

Declarations

Ethics approval and consent to participate
This research was approved by the Ethics Committee of the First Affiliated Hospital of Guangxi Medical University. The study protocol conforms to the ethical guidelines of the 1975 Declaration of Helsinki.

Consent for publication
Not applicable.

Competing interests
The authors declare no competing interests.

Received: 1 July 2024 / Accepted: 4 August 2024
Published online: 14 August 2024

References

1. Thijs RD, Surges R, O'Brien TJ, Sander JW. Epilepsy in adults. Lancet. 2019;393(10172):689–701.
2. Caciagli L, Paquola C, He X, Vollmar C, Centeno M, Wandschneider B, et al. Disorganization of language and working memory systems in frontal versus temporal lobe epilepsy. Epilepsia. 2022;63:36.
3. Hernández G, Sala-Padró J, Adell V, Rico I, Gasa-Roqué A, Morandeira F et al. Cognitive decline in adult-onset temporal lobe epilepsy: insights from aetiology. Clin Neurol Neurosur. 2024;237.
4. Pan LP, Wu YK, Bao J, Guo DD, Zhang X, Wang JJ et al. Alterations in neural networks during Working Memory Encoding related to cognitive impairment in temporal lobe Epilepsy. Front Hum Neurosci. 2022;15.
5. Bell B, Lin JJ, Seidenberg M, Hermann B. The neurobiology of cognitive disorders in temporal lobe epilepsy. Nat Rev Neurol. 2011;7(3):154–64.
6. Peltola M, Kaukinen K, Basnyat P, Raitanen J, Haimila K, Liimatainen S et al. Hippocampal sclerosis is associated with celiac disease type immunity in patients with drug-resistant temporal lobe epilepsy. J Neurol. 2024.
7. Raimondo L, Oliveira IAF, Heij J, Priovoulos N, Kundu P, Leoni RF et al. Advances in resting state fMRI acquisitions for functional connectomics. NeuroImage. 2021;243.
8. Chen JYE, Glover GH. Functional magnetic resonance imaging methods. Neuropsychol Rev. 2015;25(3):289–313.
9. Girardi-Schappo M, Fadaie F, Lee HM, Caldairou B, Sziklas V, Crane J, et al. Altered communication dynamics reflect cognitive deficits in temporal lobe epilepsy. Epilepsia. 2021;62(4):1022–33.
10. Vaughan DN, Rayner G, Tailby C, Jackson GD. MRI-negative temporal lobe epilepsy a network disorder of neocortical connectivity. Neurology. 2016;87(18):1934–42.
11. Hutchison RM, Womelsdorf T, Allen EA, Bandettini PA, Calhoun VD, Corbetta M, et al. Dynamic functional connectivity: Promise, issues, and interpretations. NeuroImage. 2013;80:360–78.
12. Cavanna F, Vilas MG, Palmucci M, Tagliazucchi E. Dynamic functional connectivity and brain metastability during altered states of consciousness. NeuroImage. 2018;180:383–95.
13. Li R, Deng CJ, Wang XY, Zou T, Biswal B, Guo DN, et al. Interictal dynamic network transitions in mesial temporal lobe epilepsy. Epilepsia. 2022;63(9):2242–55.
14. Li H, Ding F, Chen C, Huang P, Xu J, Chen Z, et al. Dynamic functional connectivity in modular organization of the hippocampal network marks memory phenotypes in temporal lobe epilepsy. Hum Brain Mapp. 2021;43(6):1917–29.
15. Di X, Biswal BB. Intersubject consistent dynamic connectivity during natural vision revealed by functional MRI. NeuroImage. 2020;216.
16. Wang SP, Wen HW, Hu XP, Xie P, Qiu S, Qian YF, et al. Transition and dynamic reconfiguration of Whole-Brain Network in Major Depressive Disorder. Mol Neurobiol. 2020;57(10):4031–44.
17. Bolton TAW, Morgenroth E, Preti MG, Van De Ville D. Tapping into multi-faceted human behavior and psychopathology using fMRI Brain Dynamics. Trends Neurosci. 2020;43(9):667–80.
18. Sitnikova TA, Hughes JW, Ahlfors SP, Woolrich MW, Salat DH. Short timescale abnormalities in the States of spontaneous synchrony in the functional neural networks in Alzheimer's disease. Neuroimage-Clin. 2018;20:128–52.
19. Rocca MA, de La Cruz MH, Valsasina P, Mesaros S, Martinovic V, Ivanovic J, et al. Two-year dynamic functional network connectivity in clinically isolated syndrome. Mult Scler J. 2020;26(6):645–58.
20. Kottaram A, Johnston LA, Cocchi L, Ganella EP, Everall I, Pantelis C, et al. Brain network dynamics in schizophrenia: reduced dynamism of the default mode network. Hum Brain Mapp. 2019;40(7):2212–28.
21. Mokhtari F, Akhlaghi MI, Simpson SL, Wu GR, Laurienti PJ. Sliding window correlation analysis: modulating window shape for dynamic brain connectivity in resting state. NeuroImage. 2019;189:655–66.
22. Pang XM, Liang XL, Zhao JY, Wu PR, Li XR, Wei WT et al. Abnormal static and dynamic functional connectivity in Left and right temporal lobe Epilepsy. Front Neurosci-Switz. 2022;15.
23. Yang S, Zhang Z, Chen H, Meng Y, Li J, Li Z, et al. Temporal variability profiling of the default mode across epilepsy subtypes. Epilepsia. 2020;62(1):61–73.
24. Leonardi N, Van De Ville D. On spurious and real fluctuations of dynamic functional connectivity during rest (104, pg 430, 2015). NeuroImage. 2015;104:464–5.
25. Li Y, Zhu YY, Nguchu BA, Wang YM, Wang HJ, Qiu BS, et al. Dynamic functional connectivity reveals abnormal variability and hyper-connected pattern in Autism Spectrum Disorder. Autism Res. 2020;13(2):230–43.
26. Zhang GM, Gai B, Zhang AY, Stephen JM, Wilson TW, Calhoun VD, et al. Estimating dynamic functional brain connectivity with a Sparse Hidden Markov Model. Ieee T Med Imaging. 2020;39(2):488–98.
27. Long ZY, Liu XP, Niu YT, Shang HJ, Lu H, Zhang JY, et al. Improved dynamic functional connectivity estimation with an alternating hidden Markov model (Nov, 10.1007/s11571-022-09874-3, 2022). Cogn Neurodyn. 2023;17(5):1399.
28. Javaheripour N, Colic L, Opel N, Li M, Balajoo SM, Chand T et al. Altered brain dynamic in major depressive disorder: state and trait features. Transl Psychiat. 2023;13(1).
29. Hawrylycz MJ, Lein ES, Guillozet-Bongaarts AL, Shen EH, Ng L, Miller JA, et al. An anatomically comprehensive atlas of the adult human brain transcriptome. Nature. 2012;489(7416):391–9.
30. Zhu D, Yuan TF, Gao JF, Xu Q, Xue KZ, Zhu WS, et al. Correlation between cortical gene expression and resting-state functional network centrality in healthy young adults. Hum Brain Mapp. 2021;42(7):2236–49.
31. Buch AM, Vertes PE, Seidlitz J, Kim SH, Grosenick L, Liston C. Molecular and network-level mechanisms explaining individual differences in autism spectrum disorder. Nat Neurosci. 2023;26(4):650–63.
32. Xiao L, Tang Y, Deng C, Li J, Li R, Zhu H, et al. Differences in whole-brain metabolism are associated with the expression of genes related to neurovascular unit integrity and synaptic plasticity in temporal lobe epilepsy. Eur J Nucl Med Mol Imaging. 2023;51(1):168–79.
33. Scheffer IE, Berkovic S, Capovilla G, Connolly MB, French J, Guilhoto L, et al. ILAE classification of the epilepsies: position paper of the ILAE Commission for Classification and terminology. Epilepsia. 2017;58(4):512–21.
34. Kang JM, Cho YS, Park S, Lee BH, Sohn BK, Choi CH et al. Montreal cognitive assessment reflects cognitive reserve. BMC Geriatr. 2018;18.
35. Pfisterer U, Petukhov V, Demharter S, Meichsner J, Thompson JJ, Batiuk MY, et al. Identification of epilepsy-associated neuronal subtypes and gene expression underlying epileptogenesis. Nat Commun. 2020;11(1):5038.
36. Liang GP, Fu WL, Wang KF. Analysis of test misuses and SPSS operations in medical research papers. Burns Trauma. 2019;7(1).
37. Wang JH, Wang XD, Xia MR, Liao XH, Evans A, He Y. vol 9, 386,. GRETNA: a graph theoretical network analysis toolbox for imaging connectomics (2015). Front Hum Neurosci. 2015;9.

38. Fallahi A, Hashemi-Fesharaki SS, Hoseini-Tabatabaei N, Pooyan M, Nazem-Zadeh MR. Dynamic functional connectivity analysis using network-based brain state identification, application on temporal lobe Epilepsy. Annu Int Conf IEEE Eng Med Biol Soc. 2023;2023:1–4.
39. Feng ZB, Zhang HT, Zhou T, Yu XG, Zhang YY, Yan XY. Dynamic functional connectivity changes associated with psychiatric traits and cognitive deficits in Cushing's disease. Transl Psychiat. 2023;13(1).
40. Christiaen E, Goossens MG, Descamps B, Larsen LE, Boon P, Raedt R et al. Dynamic functional connectivity and graph theory metrics in a rat model of temporal lobe epilepsy reveal a preference for brain states with a lower functional connectivity, segregation and integration. Neurobiol Dis. 2020;139.
41. Cohen JR. The behavioral and cognitive relevance of time-varying, dynamic changes in functional connectivity. NeuroImage. 2018;180:515–25.
42. Lin PT, Zang SY, Bai Y, Wang HX. Reconfiguration of Brain Network Dynamics in Autism Spectrum Disorder based on hidden Markov Model. Front Hum Neurosci. 2022;16.
43. Zendehrouh E, Sendi MSE, Sui J, Fu Z, Zhi D, Lv L, et al. Aberrant Functional Network Connectivity Transition Probability in Major Depressive Disorder. Annu Int Conf IEEE Eng Med Biol Soc. 2020;2020:1493–6.
44. Cao BL, Chen Y, Yu RH, Chen LX, Chen P, Weng YH et al. Abnormal dynamic properties of functional connectivity in disorders of consciousness. Neuroimage-Clin. 2019;24.
45. Li YX, Ran Y, Yao MH, Chen Q. Altered static and dynamic functional connectivity of the default mode network across epilepsy subtypes in children: a resting-state fMRI study. Neurobiol Dis. 2024;192.
46. Wang XY, Lin DD, Zhao CL, Li H, Fu LY, Huang ZF et al. Abnormal metabolic connectivity in default mode network of right temporal lobe epilepsy. Front Neurosci-Switz. 2023;17.
47. Morgan VL, Chang C, Englot DJ, Rogers BP. Temporal lobe epilepsy alters spatio-temporal dynamics of the hippocampal functional network. Neuroimage-Clin. 2020;26.
48. Liang XL, Pang XM, Zhao JY, Yu L, Wu PR, Li XR, et al. Altered static and dynamic functional network connectivity in temporal lobe epilepsy with different disease duration and their relationships with attention. J Neurosci Res. 2021;99(10):2688–705.
49. Peng YQ, Wang KR, Liu CR, Tan LZ, Zhang M, He JLZ et al. Cerebellar functional disruption and compensation in mesial temporal lobe epilepsy. Front Neurol. 2023;14.
50. Wagner MJ, Luo LQ. Neocortex-cerebellum circuits for cognitive Processing. Trends Neurosci. 2020;43(1):42–54.
51. Wang G, Liu XH, Zhang M, Wang KR, Liu CR, Chen YY et al. Structural and functional changes of the cerebellum in temporal lobe epilepsy. Front Neurol. 2023;14.
52. Streng ML, Froula JM, Krook-Magnuson E. The cerebellum's understated role and influences in the epilepsies. Neurobiol Dis. 2023;183.
53. Zhou X, Chen Z, Xiao L, Zhong Y, Liu Y, Wu J, et al. Intracellular calcium homeostasis and its dysregulation underlying epileptic seizures. Seizure: Eur J Epilepsy. 2022;103:126–36.
54. Ren E, Curia G. Synaptic reshaping and neuronal outcomes in the temporal lobe Epilepsy. Int J Mol Sci. 2021;22(8).
55. Ng AC, Chahine M, Scantlebury MH, Appendino JP. Channelopathies in epilepsy: an overview of clinical presentations, pathogenic mechanisms, and therapeutic insights. J Neurol. 2024;271(6):3063–94.
56. Maganti RK, Jones MV. Untangling a web: Basic mechanisms of the complex interactions between sleep, circadian rhythms, and Epilepsy. Epilepsy Curr. 2021;21(2):105–10.
57. Patel DC, Tewari BP, Chaunsali L, Sontheimer H. Neuron-glia interactions in the pathophysiology of epilepsy. Nat Rev Neurosci. 2019;20(5):282–97.
58. Roy A, Skibo J, Kalume F, Ni J, Rankin S, Lu Y et al. Mouse models of human PIK3CA-related brain overgrowth have acutely treatable epilepsy. Elife. 2015;4.
59. Ghafouri-Fard S, Hussen BM, Jamali E, Branicki W, Taheri M. Akbari Dilmaghani N. Role of lncRNAs and circRNAs in Epilepsy. Ageing Res Rev. 2022;82:101749.
60. Hodges SL, Lugo JN. Wnt/beta-catenin signaling as a potential target for novel epilepsy therapies. Epilepsy Res. 2018;146:9–16.

Publisher's Note